

APPLICATION OF DETONATION SHOCK DYNAMICS TO THE PROPAGATION OF A DETONATION IN NITROMETHANE IN A PACKED INERT PARTICLE BED

David L. Frost¹, Tariq Aslam², and Larry G. Hill²

¹*McGill University, Department of Mechanical Engineering, 817 Sherbrooke St. W., Montreal, Quebec, Canada H3A 2K6*

²*Los Alamos National Laboratory, Los Alamos, NM 87544*

Abstract. A multidimensional implementation of DSD, formulated with the level set method, is applied to track the propagation of a detonation wave in a heterogeneous explosive consisting of an array of inert cylindrical obstacles with a liquid explosive in the interstitial space. With the Huygens assumption, the average detonation velocity through the explosive is less than that for the liquid explosive alone, due to the increased path length. When the normal detonation velocity is assumed to depend on front curvature, there is an additional, smaller reduction in the detonation velocity, which depends on the cylinder material. The detonation velocity deficits obtained in the computations are of the same order as those observed experimentally for a heterogeneous explosive consisting of a packed bed of spherical inert beads saturated with sensitized nitromethane. The DSD computations are relevant to the experimental results in the large-bead limit in which the pore dimension is large enough to support the propagation of discrete detonation wavelets in the interstitial liquid between the beads.

INTRODUCTION

When inert particles are added to a liquid explosive such as nitromethane (NM), the detonation velocity and pressure are reduced since a portion of the chemical energy released goes to heating and accelerating the inert material. Adding a small number of inert heterogeneities such as solid particles (1) or microballoons (2) to NM also leads to a large increase in the sensitivity of NM. This sensitizing effect is due to the generation of hot-spots as a result of the interaction of the shock wave with the heterogeneities. For a heterogeneous explosive consisting of NM with a large volume fraction of inert material, evidence exists that hot-spot generation due to shock diffraction and collisions also plays a role (3).

Lee et al. (4) found that for a packed bed of inert monodisperse spherical beads saturated with sensitized NM, two distinct propagation mechanisms can occur, depending on the bead

diameter. The heterogeneous explosive is most insensitive (i.e., the failure diameter reaches a maximum) when the bead diameter is a critical value, which is on the order of the failure diameter for the pure liquid explosive. For bead diameters less than the critical value, the detonation fails to propagate around the beads, but instead the shock propagation through the beads is sufficient to initiate the explosion of the liquid in the interstitial pores. In this “small-bead” regime, as the bead size decreases, the density of artificial hot-spots associated with the beads increases and the failure diameter decreases. A different behavior is observed if the bead diameter is larger than the critical value. In this case, the global detonation propagation is controlled by the propagation of local detonation wavelets in the pores between the beads. In this “large-bead” regime, as the bead size increases, diffraction effects become less severe and hence the failure diameter of the mixture decreases (4). When the bead diameter is near the critical value, shock

propagation through the beads and propagation of a reactive front in the interstitial liquid both play a role in the overall propagation mechanism. In this case, highly resolved hydrocode calculations, with a realistic model for the NM reaction rate, are necessary to resolve the propagation mechanism. However, in the limits of very small and very large beads, simpler analytical approaches can be considered. In the small-bead regime, as the bead size approaches zero, the beads will be in mechanical and thermal equilibrium with the combustion products within the reaction zone. Hence the inert beads will act as a diluent and equilibrium Hugoniot calculations are expected to give a reasonable prediction of the resulting detonation velocity and pressure. In the large-bead regime, discrete detonation wavelets will propagate around the beads. If the radius of curvature of the detonation front is large compared with the characteristic reaction zone thickness of the wave, then detonation shock dynamics (DSD) theory can be used to track the propagation of the detonation front through the heterogeneous explosive.

In the present paper the experimental results for the detonation velocity of the heterogeneous explosive are first presented. The detonation propagation in the limits of small and large beads are then explored with equilibrium Hugoniot and DSD calculations, respectively. The simplest form of DSD theory is used, in which the normal detonation shock velocity, D_n , is a function of the local total shock curvature, κ . A multidimensional implementation of DSD, formulated with the level set method (5), is used to track the propagation of the detonation front through a regular array of inert obstacles. The effects of geometry, $D_n(\kappa)$ relation, and bead material on the average propagation velocity are determined.

RESULTS AND DISCUSSION

Experimental Results

In general, the average propagation velocity of a detonation wave through a packed bed of spherical particles saturated with liquid explosive is less than the detonation velocity of the liquid explosive itself. Lee (3) observed detonation velocities (extrapolated to infinite charge diameter) in the range of 4.2–4.6 km/s for glass beads ranging in size from 66 μm to 2.4 mm saturated with NM

sensitized with 15% DETA, as compared with a detonation velocity of about 5.8 km/s for the liquid, as computed with the equilibrium code CHEETAH (6). For glass beads with a mean diameter of 2.4 mm, which corresponds to the large-bead regime, Lee (3) estimated the infinite charge diameter detonation velocity to be about 4.5 km/s (i.e., $D/D_{CJ} = 0.78$). With metal beads, Lee (3) found that the detonation velocity in the large-bead regime increased to about 4.8 km/s (i.e., $D/D_{CJ} = 0.82$).

The average detonation velocity in the large-bead regime is typically larger than that for the small-bead regime. However, within each propagation regime, the detonation velocity, extrapolated to infinite charge diameter, is approximately the same, independent of bead diameter. This is illustrated in Fig. 1, which shows the diameter effect curves for heterogeneous charges with beads of various diameters. The results shown in Fig. 1 are an extension of earlier work in which steel beads were used with the less sensitive explosive mixture NM + 10% triethylamine (TEA), which has a failure diameter of about 2.6 mm with glass confinement as compared to about 1 mm for NM + 15% DETA (7). The extrapolated detonation velocities in the small- and large-bead regimes are, respectively, about 3.9 and 5.1 km/s, or 68% and 89% of the value of D_{CJ} of 5.7 km/s calculated with CHEETAH (6) for the liquid explosive alone.

Equilibrium Calculations: Small-Bead Regime

Also shown in Fig. 1 is the detonation velocity calculated using CHEETAH (6) for a mixture of iron and NM + 10% TEA. Although the EOS formulation is not expected to be accurate for an explosive with such a high mass fraction of inert material, if we extrapolate the calculated values of D_{CJ} , plotted as a function of iron mass fraction, to the experimental value (91%), we obtain a D_{CJ} of about 2.3 km/s, considerably less than the experimental value of 3.9 km/s. This is expected since the assumption that the beads are in thermal and mechanical equilibrium with the combustion products at the CJ plane is not valid for the particle sizes used in the experiments. To obtain a more accurate estimate of the detonation velocity in the small-bead regime it is necessary to explicitly account for the momentum and energy exchange between the beads and combustion products.

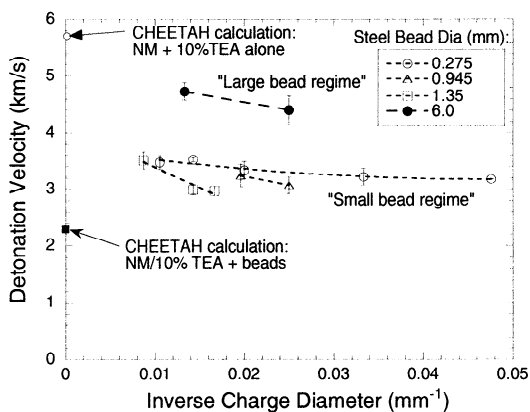


FIGURE 1. Effect of bead size on the diameter effect curve for a heterogeneous explosive consisting of a packed bed of steel beads (91% steel by mass) saturated with NM + 10% TEA.

DSD Calculations: Large-Bead Regime

To gain insight into the propagation of the detonation in the large-bead regime, DSD calculations were carried out to track the propagation of detonation wavelets around an array of inert objects. In the experiments with a packed bed of spherical beads, although the average solid volume fraction is about 60%, the actual packing geometry of the beads is not known. Given the uncertainty in the bead packing, the simpler problem of the propagation of a detonation through a regular 2-dimensional array of cylinders was considered. The propagation of a detonation through a 2-dimensional array of cylinders will be qualitatively, although not quantitatively, similar to detonation propagation through a regular array of spheres.

If we make the so-called Huygens assumption, in which the detonation velocity in the liquid is assumed to be constant, independent of front curvature, then the maximum propagation velocity through the array will correspond to the shortest path length through the array, which can be determined analytically. Figure 2 shows a regular array of cylinders or radius r with spacing d in which the shortest path length through the array is shown. By determining this path length from geometrical considerations, the ratio of the average detonation velocity through the array to the

detonation velocity in the liquid, D_{avg}/D_{CJ} , can be determined, and is shown in Fig. 3 as a function of the ratio of cylinder radius to spacing r/d . If we consider an array of cylinders with the same solid volume fraction as the experiments with beads (i.e., 60% corresponding to $r/d = 0.407$), we obtain $D_{avg}/D_{CJ} = 0.933$.

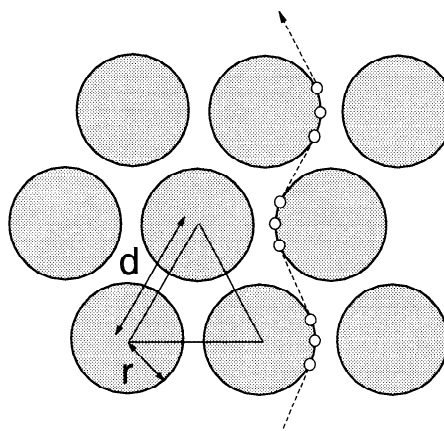


FIGURE 2. Shortest path length (dashed line) through a regular array of cylinders with radius r and spacing d .

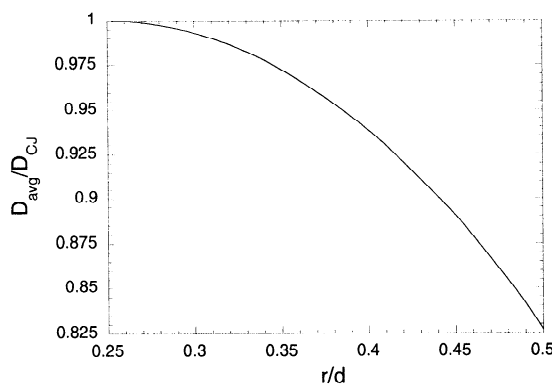


FIGURE 3. Ratio of average detonation velocity through regular array of cylinders D_{avg} to D_{CJ} of liquid as a function of cylinder radius/spacing ratio calculated considering shortest path length through cylinders shown in Fig. 2.

Calculations were then carried out with the DSD code to track the detonation propagation through an array of cylinders with a solid volume fraction of 60%. From symmetry considerations, it is sufficient to track the propagation through a staggered array of half-cylinders. In Fig. 4 the detonation fronts are shown at various times during the propagation. With the Huygens assumption,

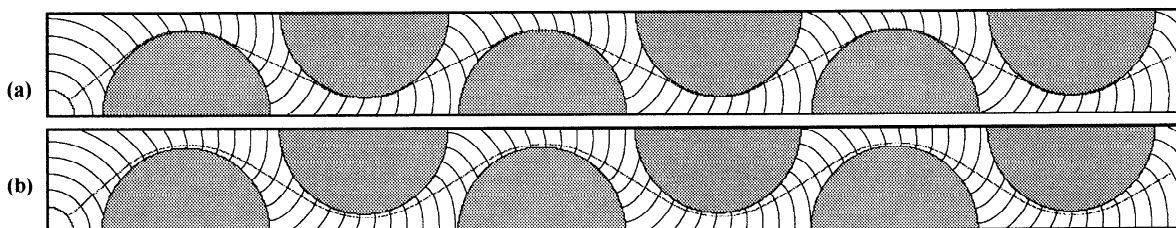


FIGURE 4. Detonation wavefronts and shortest path (line) through a staggered array of cylindrical obstacles computed with DSD code with (a) the Huygens assumption, and (b) using $D_n(\kappa)$ for NM + 15% DETA with glass cylinders.

the normalized average detonation velocity through the array is found to be $D_{avg}/D_{CJ} = 0.931$, which agrees, within numerical error, with the analytical calculation above.

To investigate the influence of front curvature on the propagation, the 2-d calculations were repeated, with the assumption that the local normal detonation velocity D_n was a nonlinear function of front curvature, κ , as given by equation (5) of Hill et al. (8) with the following parameters: $D_{CJ} = 5.8211 \text{ mm}/\mu\text{s}$, $\kappa_f = 2.3981 \text{ mm}^{-1}$, $b_1 = 0.04698$, $b_2 = 0.2749$, $b_3 = 0.01525$, $b_4 = 0.002762$, $b_5 = 0.741$, $b_6 = 0.6135$, and $b_7 = 0.2398$. For $\kappa < 0$, a linear $D_n(\kappa)$ relation was used, with the same slope as that at $\kappa = 0$. For $\kappa > 2.398$, then $D_n = D_n(\kappa = 2.398)$. A bead diameter of 6 mm was used, which corresponds to the large-bead regime for both glass and steel beads. A sonic angle (5) of 56° was used and critical angles for glass and steel confinement of 62° and 86° , respectively, were used (9).

The results of the computations are shown in Table 1. With the Huygens assumption, the average detonation velocity deficit (relative to D_{CJ}) is 7% as a result of the increased geometrical path length. When the local front velocity is considered to be a function of wavefront curvature, then a further velocity deficit of between 3 or 4% is introduced, depending on whether steel or glass

cylinders are present. The trends with respect to bead material are the same as those observed experimentally, i.e., steel beads provide a more rigid confinement for the wave and the wave propagates at a higher speed past the steel obstacles than for glass obstacles. Future calculations will consider the propagation through a 3-dimensional array of inert spheres to more closely reproduce the actual geometry of the experiments.

ACKNOWLEDGMENTS

The experimental results (Fig.1) were obtained with the assistance of H. Kleine and the technical staff of the Canadian Defense Research Establishment Suffield. Useful comments provided by J. Bdzil and R. Engelke are also gratefully acknowledged.

REFERENCES

- 1) Campbell, A. W., Davis, W. C., and Travis, J. R., *Phys. Fluids* **4**, 498-510 (1961).
- 2) Presles, H. N., Campos, J., Heuze, O. and Bauer, P., "Effects of Microballoons Concentration on the Detonation Characteristics of Nitromethane-PMMA Mixtures," in *9th Symp. (Int.) on Detonation*, OCNR 113291-7, Portland, OR, 1989, 925-929.
- 3) Lee, J. J., "Detonation Mechanisms in a Condensed-Phase Porous Explosive," Ph.D. thesis, Université de Sherbrooke, (1997).
- 4) Lee, J. J., Frost, D. L., Lee, J. H. S., and Dremin, A., *Shock Waves* **5**, 115-119 (1995).
- 5) Aslam, T. D., Bdzil, J. B., and Stewart, D. S., *J. of Comp. Phys.* **126**, 390-409 (1996).
- 6) Fried, L. E., Howard, W. M., and Souers, P. C., "Cheetah 2.0 User's Manual," LLNL, UCRL-MA-117541 Rev. 5, (1998).
- 7) Radulescu, M., "Influence of Confinement on the Detonation Properties of a Liquid Explosive," B. Eng. (Hon.) thesis, McGill University, (1997).
- 8) Hill, et al., These Proceedings (1999).
- 9) Bdzil, J. Private Communication, (1999).

TABLE 1. Average Detonation Velocity for Propagation through an Array of Cylinders with a Solid Volume Fraction of 60%.

Model	D_{avg}/D_{CJ}
1) Analytical "minimum path length"	0.933
2) DSD w/Huygens assumption	0.931 ± 0.003
3) DSD w/ $D_n(\kappa)$ for sensitized NM (15% DETA) w/steel cylinders	0.902 ± 0.002
4) DSD w/ $D_n(\kappa)$ for sensitized NM (15% DETA) w/glass cylinders	0.888 ± 0.003